TÜBİTAK

Turkish Journal of Earth Sciences

http://journals.tubitak.gov.tr/earth/

Research Article

Turkish J Earth Sci
(2023) 32: 113-125

doi:10.55730/1300-0985.1830

Hydrogeochemical pattern and environmental isotope hydrology of coastal Bademli geothermal area (BGA) in western Turkey (Dikili-İzmir): A new geothermal prospect

Melis SOMAY-ALTAŞ*, Ünsal GEMİCİ
Department of Geological Engineering, Dokuz Eylül University, İzmir, Turkey

Received: 21.06.2022 • **Accepted/Published Online:** 15.12.2022 • **Final Version:** 19.01.2023

Abstract: Bademli geothermal area (BGA) is located on the coastline of Dikili-İzmir province and consists of Bademli spring and Hayıtlı areas with 36.8–51°C discharge temperatures, respectively. The waters of Hayıtlı borehole have remarkable seawater mixing ratios like Bademli spring and have Na-Cl water type. Dikili group pyroclastic volcanic units constitute the reservoir rock in the entire geothermal area. The heat source is relatively elevated geothermal gradient caused by extensional tectonics forming E-W trending grabens. Bademli thermal water is plotted in the "immature waters" area in the Na-K-Mg triangular diagram with a calculated seawater contribution of 18%. Therefore, some cation geothermometers are considered unreliable. On the other hand, the silica-enthalpy diagram showed an anticipated reservoir temperature of approximately 240 °C. Hayıtlı borehole water sample is plotted on the "partially equilibrated waters" area in the same triangular diagram and shows a reservoir temperature of 208 °C. The seawater contribution in the Hayıtlı area (16%) is less than the Bademli spring. On the other hand, based on the K/Mg geothermometry, the reservoir temperatures for Bademli spring and Hayıtlı borehole waters are 129 °C and 138 °C, respectively. B, Fe, Mn, and Sb concentrations exceed the tolerance limits of the EPA and Turkish drinking water standards in the area. In addition, due to silica-rich volcanic rocks, Ge solubility increased with temperature in thermal waters and reached 34–45 µg/L. Enrichment of $\delta^{18}O$ and $\delta^{2}D$ values can be observed in Bademli spring and Hayıtlı with −3.70‰ and −4.63‰, and −34.5‰ and −37.9‰, respectively. From the chemical and isotopic results, it can be clearly said that this coastal geothermal area is high enthalpy, as evident from the equilibrium temperatures. However, when the thermal water rises to the surface, it mixes with both cold groundwater and modern seawater resulting in a decrease of the discharge temperatures of the springs. Moreover, according to the isotopic and hydrogeochemical data, the area has a high potential for thermal heating of the settlements in the area.

Key words: Geothermal, hydrogeochemistry, isotopes, Bademli, Dikili, Turkey

1. Introduction

Geothermal energy is a sustainable and renewable energy source that uses the heat of the earth's crust. Water and/or steam carry geothermal energy as thermal fluids to the earth's surface. These fluids contain more dissolved minerals, salts, and gases than the groundwater have temperatures above those of the regional atmospheric temperatures. Since the waters forming the geothermal fluid are generally of meteoric origin, geothermal resources are renewed as long as the atmospheric conditions continue. Geothermal energy does not create air pollution with its low carbon dioxide emission rate and is a renewable alternative energy source. Geothermal energy is a clean, inexpensive, and environmentally friendly resource (Yang et al., 2017; Çetin et al., 2021). It does not cause carbon emissions and air pollution in the atmosphere. Hot dry rocks without water are also geothermal energy sources.

Western Anatolia is where 78% of Turkey's geothermal potential is found. The remaining 9% is in Central Anatolia, 7% in Marmara, and 6% in Eastern Anatolia. According to Ministry of Energy and Natural Resources of Turkey data, 90% of geothermal resources are suitable for direct applications (low and medium temperature) such as various industrial applications, thermal tourism, and heating, etc. while the remaining 10% is suitable for indirect applications such as electricity generation (high temperature) (MAGEG, 2022). Investigation of the geothermal system in Turkey, development, exploitation, and conservation is of great importance. It should never be forgotten that, if geothermal energy is not protected, it will not have the same efficiency in the future and may even disappear completely. Since these waters are healing in terms of health, it is of particular importance that their hydrogeochemical properties remain intact.

* Correspondence: melis.somay@deu.edu.tr

The geothermal activity is thought to have been enriched by the behavior of Western Anatolia during the Neogene and by the extensional tectonics in the region that caused the formation of the grabens (Simsek, 2003). These grabens are Bakırçay, Gediz, Küçük Menderes, and Büyük Menderes grabens from north to south. Many researchers have been studying the hydrogeology and hydrogeochemistry of these grabens for many years (Eşder and Şimşek, 1977; Filiz, 1982; Yılmazer, 1984; Güleç, 1988; Balderer and Synal, 1996; Karamanderesi, 1997; Özgür, 2002; Vengosh et al., 2002; Gemici and Tarcan 2002; Baba et al, 2006; Mutlu et al, 2008; Magri et al., 2011; Bülbül et al., 2011; Özen et al, 2012; Alçiçek et al., 2018; Tut-Haklıdır and Özen-Balaban; 2019; Akar et al, 2021).

İzmir province is quite rich in terms of geothermal fields (İZKA, 2022). There are the Çeşme geothermal area (62 ℃- Gemici and Filiz,2001), Seferihisar geothermal area (153 ℃- Tarcan and Gemici, 2003), Aliağa geothermal area (51 ℃- Filiz et al. 1997; Özkan et al, 2011), Dikili-Kaynarca geothermal area (150–200 ℃- Özen and Tarcan, 2005), Bergama geothermal area (25–58 ℃- Filiz et al. 1998), Bayındır geothermal area in the (42–46 ℃- Bulut and Filiz, 2005), Urla-Gülbahçe geothermal area (37 ℃- Filiz and Tarcan, 1990), and in the city Balçova-Narlıdere geothermal area (95–140 ℃-Tarcan et al. 2009).

Geothermal energy sources are used in İzmir city for thermal tourism and regional heating. Most of the geothermal energy used in İzmir province is used in residential heating. Residential heating consumes 59% of the total energy, greenhouse heating consumes 36%, and thermal tourism uses the final 5%. (Aksoy, 2014; İZKA, 2022).

Dikili-Bergama geothermal fields located northern part of Bakırçay Basin is one of Turkey's major geothermal fields. Bademli geothermal area (BGA) is located northern part of İzmir city which is the third biggest city in Turkey (Figure 1). Another important geothermal area (Dikili Geothermal Area) is used for thermal production eastern part of BGA. Agriculture, green housing, and tourism are the main sources of income in Dikili, İzmir (Ataberk and Baykal, 2011). Bademli village is one of the most important tourist locations in Dikili. Especially thermal tourism has a very important position in the region. There are hotels with a bed capacity of approximately 1700. Geothermal

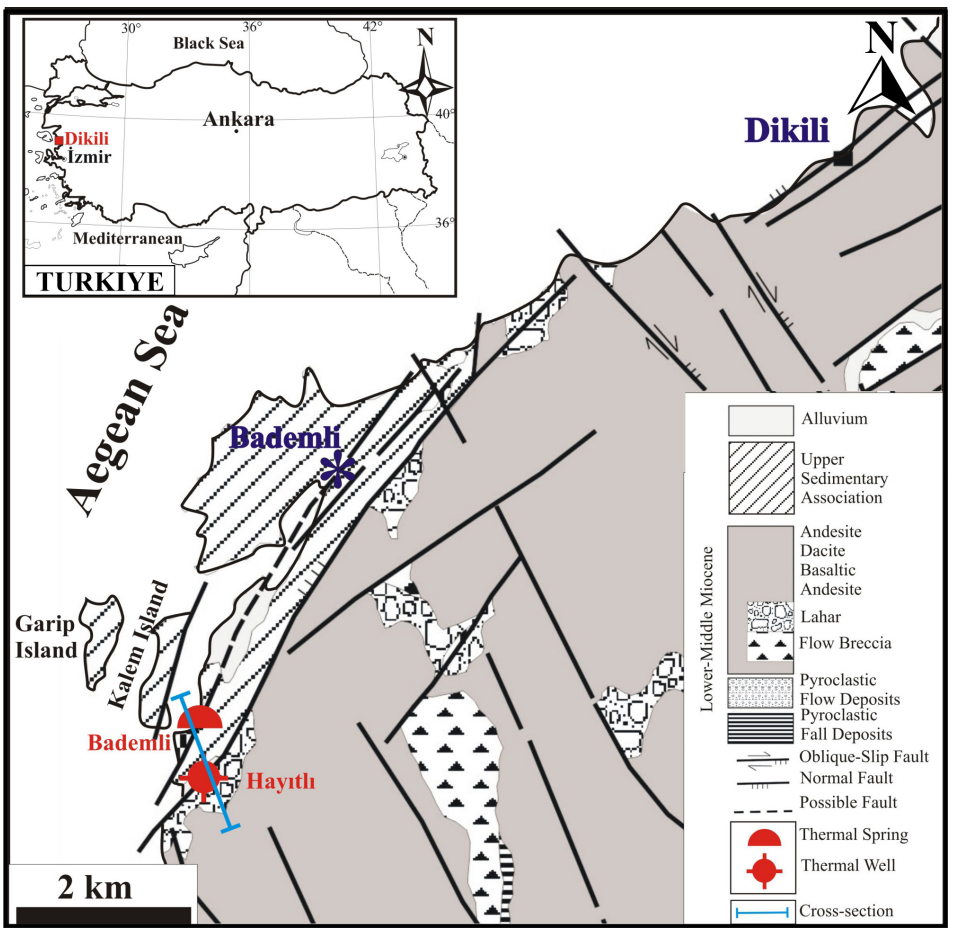

Figure 1. Location and geological maps of the study area (Karacık et al., 2007).

research is being carried out for new tourism opportunities both in this area and in the two nearby islands (Kalem and Garip Islands).

There is a limited detailed hydrogeochemical study in BGA. The purpose of this investigation is to evaluate the hydrogeological and hydrogeochemical properties of BGA thermal waters, their relations with groundwater, and the application of chemical geothermometers. In addition, an investigation of the heavy metals as boron contents of water was done to determine the environmental problems.

2. Material and methods

Studies can be divided into two groups: field and laboratory studies. The cold groundwater and thermal waters were sampled in 2015 in the study area. The pH, electrical conductivity (EC), and temperature measurements of the waters were made in situ with a WTW multimeter. The HCO_3 values of the waters were determined in the field by in situ titration method. Water samples for chemical analysis were filtered through 0.2-µ permeable filter paper with the help of a water filtration set into 50 mL and 500 mL polyethylene bottles. Water samples were acidified to a pH of 2 by adding 0.2 mL of concentrated HNO_3 to the sample bottles (50 mL) in which cation analyzes would be made. The waters were stored at +4 °C as specified in the standards and sent to ACTLab in Canada for cation analyses. Anion analyzes were performed in the Dokuz Eylül University Geological Engineering Geochemistry Laboratory. HCO_3 and Cl ions were done with the volumetric, and SO_4 was done with the gravimetric method according to APHA-AWWA-WCPF, 1992. One 50 mL water sample bottle was used for $\delta^{18}O$ and $\delta^{2}D$ analyzes of water. $\delta^{18}O$ and $\delta^{2}D$ analyzes were performed at the University of California, Davis Laboratory in the USA. AquaChem 5.1 (Calmbach, 1997) computer code was used to evaluate hydrogeochemical and PhreeqC (Parkhurst and Appelo 1999) chemical speciation programs.

3. Geology and hydrogeology

At the basement of the study area, there are Early-Middle Miocene aged pyroclastic rocks called both Yuntdağı Volcanic Units (Akyürek and Soysal, 1983) and Dikili group (Karacık et al., 2007), andesitic, dacitic lavas, lava breccias and lahar flows (Figure 1). It crops out in an area of approximately 45 km^2 in the study area. It often has flowing lava structures that present a layering appearance. Andesite units in the region have cracks and fracture systems that allow their circulation and storage. The shallow water wells drilled in the andesite unit are for drinking, and irrigation purposes; and their depths vary between 4–20 m. In addition, recharge rates change from 0.1 to 0.4 l/s (Demirel, 1993). The Dikili group forms the reservoir rock of the Bademli geothermal system.

Middle Miocene-Lower Pliocene age Soma Formation, which overlies the rocks of the Dikili group, covers approximately 8 km^2 of the study area. At the bottom of the Soma formation, large blocks, gravel, and clays belonging to the foundation are dominant. Clay-sand-sandstones are dominant towards the upper parts, and greenish plastic clay level is dominant in the uppermost parts. Marl is dominant in the upper levels of the formation. In addition, it is possible to observe transition units between limestone bands and marl-limestone (Akyürek and Soysal, 1983). Marl is of medium hardness and is bluish-gray in color. It shows very well bedding; the layers can reach 1–2 m thick from the lamina. Because of the predominance of clayey impermeable layers, the Soma formation forms the cover rock of the BGA.

Quaternary alluvium covers all units in the region uncomfortably. It covers approximately 2.5 km^2 in area. The thickness of the alluvium varies between 2–4 m near the coast and 15–20 m on the land (Demirel, 1993).

4. Results

4.1. Hydrogeochemistry

The chemical analysis results of three water samples taken from three different water points were determined in the study area (Table 1). The surface temperature and pH values of Bademli geothermal spring (sample 1) and Hayıtlı borehole (sample 2) are between 36.8 and 51.0 °C and 6.58 and 6.81, respectively. The well bottom temperatures were measured at 96 °C at 160 m. The EC value of the geothermal fluid is between 11,090 and 10,420 µS/cm, and its average value is 10,755 µS/cm. The cold groundwater sample taken from Bademli Village (sample 3) was measured at 22 °C, pH value of 7.12, and an electrical conductivity value of 515 µS/cm.

The analysis results obtained by determining the chemical characteristics of the geothermal fluid provide information about the relations of the geothermal fluid with lithology and the hydrogeochemical processes that occur throughout the circulation systems. Thermal waters have total dissolved solids (TDS) values of 7000–7400 mg/L. The major cation sequence of the geothermal fluid is $Na^+ > Ca^{+2} > K^+ > Mg^{+2}$, and the anion sequence is $Cl^- > HCO_3^- > SO_4^{-2}$. Although the Mg concentration in seawater is high, the concentration of Mg in geothermal water, which is a seawater additive, is lower than that of calcium. This situation can be explained by ion exchange reactions that cause the magnesium value to decrease in the mixture between magnesium, calcium, and sodium.

The salinization of groundwater with the addition of seawater is essentially the mixing of fresh groundwater (unsalted) with seawater. In hydrogeological studies, mixture amounts are calculated using physically or chemically nonreactive components (e.g., Cl, EC). The

determination of components that provide this mixture, the result of the hydrogeochemical mixture of the two end components, can be determined by using the volumetric ratios of the end components in water with the following equation:

$$\text{Contribution of end component (\%)} = \frac{Cl_{sample} - Cl_{fresh}}{Cl_{sea} - Cl_{fresh}}$$

Equation (1)

According to equation 1, mixing ratios of thermal waters are calculated with Cl, Na, Mg, and EC values of the samples. The cold-water sample was used as a "freshwater end component". As a result, the mixture ratios calculated according to all these values were found 18% for Bademli spring and 16% for Hayıtlı borehole. In support of all these results, the water type of geothermal water is Na-Cl, while the cold groundwater is Ca-Mg-Na-HCO_3-Cl according to IAH's (1979) classification.

The chemical analysis results were plotted on the Piper diagram to determine the hydrogeochemical facies of the waters in the study area (Figure 2).

According to this diagram, geothermal waters are located in the Na-K-Cl type waters type (noncarbonate alkali-primary salinity exceeds 50%). Cold groundwater is Ca-Mg-Na-HCO_3 water type (carbonate hardness exceeds 50%). Na is the dominant cation for thermal waters in BGA according to Piper Diagram and IAH (1979) classification. Na concentration is on average 2100 mg/L for thermal waters. However, the Na value is much lower for cold groundwater (28 mg/L). Na-rich thermal waters are produced by seawater intrusion in the area.

According to the Schoeller semilog diagram, the parallelism of the lines shows that the fluid has a similar ion to the recharge area and reservoir. As shown in the Schoeller semilog diagram (Figure 3) geothermal

Table 1. Chemical analyses of the waters (EC = Electrical conductivity; T = Temperature; major ions units are mg/L* Somay et al. 2008).

#	Location	EC (µS/cm)	T (°C)	pH	Na^+	K^+	Ca^{+2}	Mg^{+2}	Cl^-	HCO_3^-	SO_4^{-2}	Si	Water Type (IAH. 1979)	δ^2D (‰)	$\delta^{18}O$ (‰)
1	Bademli thermal spring	11,090	36.8	6.58	2,263	189.90	184	38	3,850	683	298	89.8	Na–Cl	–34.5	–3.70
2	Hayitli thermal borehole	10,420	51.0	6.81	2,138	187.40	177	21	3,725	537	252	93.1	Na–Cl	–37.9	–4.63
3	Bademli cold GRW	515	22.0	7.12	27	0.02	39	16	34	183	4	49.7	Ca–Mg–Na-HCO_3–Cl	–36.4	–6.66
SW*	Seawater	58,800	17.0	8.28	12,720	399.00	413	1,381	21,702	156	2,379	0.5	Na–Cl	8.4	1.61

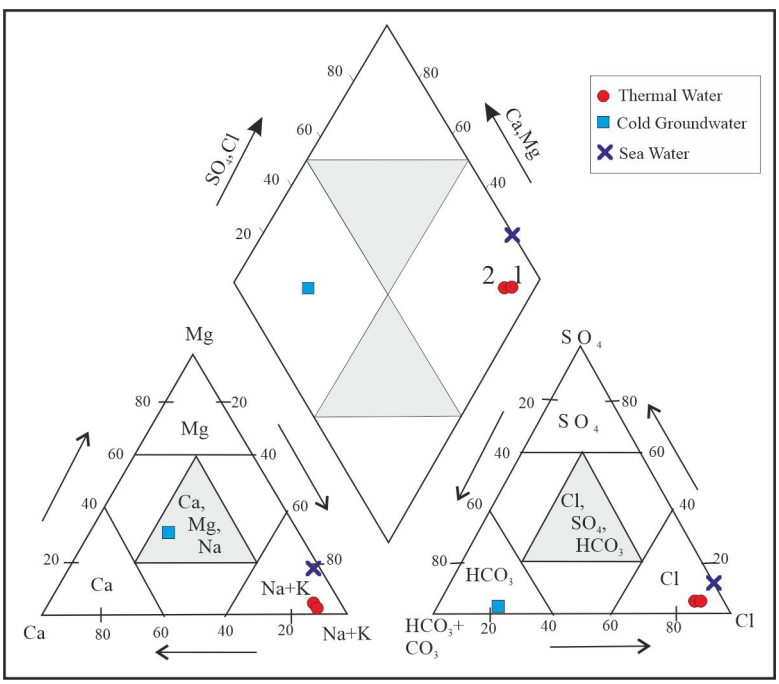

Figure 2. Distribution of thermal waters in Piper diagram.

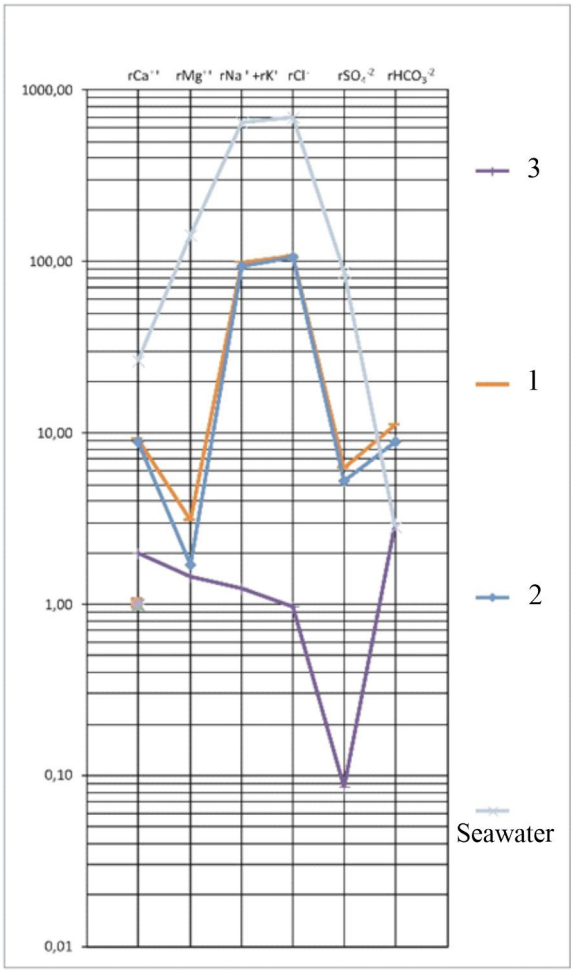

Figure 3. Distribution of waters in Schoeller semilog diagram.

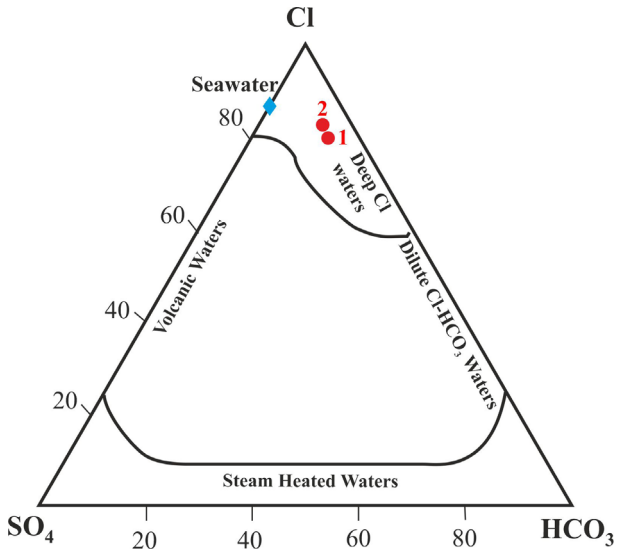

Figure 4. Cl-SO_4-HCO_3 ternary diagram.

borehole and spring are in a parallel sequence and show the seawater effect in the BGA. According to the Schoeller semilogarithmic diagram, the dominant ion distribution in geothermal waters is Na+K>Ca>Mg for cations and Cl >HCO_3> SO_4 for anions. The dominant ion distribution in cold groundwater is Ca>Mg>Na+K for cations and HCO_3>Cl>SO_4 for anions.

Thermal waters can be distinguished on the Cl-SO_4 -HCO_3 ternary diagram of Giggenbach's (1991) diagram (Figure 4). This diagram shows that the thermal waters in the region are classified as "deep Cl waters".

Boron concentrations in thermal waters reach 45.7 mg/L (Table 2). Mixing of thermal waters with groundwater and surface waters may cause some environmental problems. Although boron is the basic element for the growth of plants, if the limit value is exceeded, the plants die and accumulate causing the soil to become barren. If the boron concentration in groundwater exceeds 1 mg/L, it is harmful to plants (Richards, 1954). More amounts of boron in thermal waters are caused boric acid dissolution so fast and affect living things negatively.

High concentrations of iron, manganese, and antimony are related to geothermal activity in the area. An increase in germanium content is observed in thermal groundwaters in bedrocks made of reactive silicate minerals. These silicate minerals are especially found in active volcanic regions and/or in young igneous rocks (Dobrzynski et al. 2018). Mineralogy, geochemistry, and temperature of reservoir rock can be affected by the germanium concentration in thermal waters. With the increase in temperature, the total solubility of GeO_2 and silica also increases (Wood and Samson, 2006). Some measured Ge concentrations in thermal waters are shown in Table 3.

Since the silica-rich acidic volcanic formations, which are common in the Dikili-Çandarlı region, form the reservoir rock of the geothermal area, it is normal for the germanium solubility to increase in the waters.

4.2. Environmental isotope hydrology

Effective and beneficial use of water resources is possible by determining recharge areas and understanding their circulation. Stable Oxygen ($\delta^{18}O$) and Deuterium ($\delta^{2}D$) isotopes are generally used to determine the geothermal fluid origins (meteoric, fossil, etc.), recharge areas, and the temperature of the fluid in the aquifer. The isotope values of all other waters are measured according to Standard Mean Ocean Water (SMOW), where the δ value is assumed to be zero. Environmental isotope analyzes of water samples in the study area are presented in Table 1. The stable $\delta^{18}O$ and $\delta^{2}D$ isotopes are generally used to determine the origin of the waters, the recharge level and area, and the temperature in the aquifer. The linear relationship between

Table 2. Some minor ions of waters (underlined values exceed standards).

#	Location	Al (µg/L)	B (µg/L)	Fe (µg/L)	Ge (µg/L)	Mn (µg/L)	Sb (µg/L)	Zn (µg/L)
1	Bademli thermal spring	10	44,700	600	34.20	141.0	22.8	45.9
2	Hayıtlı thermal borehole	8	45,700	500	45.20	260.0	115.0	427.0
3	Bademli cold GRW	5	nm	20	0.33	0.3	0.1	29.9
	EPA standards (2014)	50–200	2000	300	–	50	6	5000
	TSE-266 (2005)	200	2000	300		50	5	–

Table 3. Some measured Ge concentrations in thermal waters.

Area	Unit µg/L	Reference
France-Vichy thermal area	25	Bardet, 1914
Japan-Senami thermal area	30	Kuroda, 1939
New Zealand thermal areas	52	Koga, 1967
Poland thermal areas	1.01	Dobrzynski et al. 2018
Eastern Turkey thermal areas	24	Pasvanoğlu, 2020
Bademli geothermal area	34–45	This study

values of precipitation isotopes depends on mainly climatic conditions and is expressed by the relation $\delta^2D = \alpha\delta^{18}O+d$. These values, throughout the hydrological cycle; vary depending on evaporation, humidity, precipitation, climatic conditions, and geographical location. For this reason, local meteoric water lines are available for many regions based on regional precipitation. These meteoric water lines are used to determine the origin of groundwater. Dilaver et al., 2018 data was used as a local meteoric line with $\delta^2D = 8\delta^{18}O+12$ for the study region (Figure 5).

According to the isotope analysis results made at the thermal and cold-water sample points in the study area, the $\delta^{18}O$ and δ^2D values in the waters vary between –3.70 ‰ and –6.66 ‰ and –35.5 ‰ and –37.9 ‰, respectively. In Figure 5, according to the $\delta^{18}O$ and δ^2D isotope results, it is seen that the thermal waters are displaced to higher oxygen isotope ratios due to water-rock interaction. In the diagram, it is clearly seen that the waters in BGA are located to the right of the meteoric water line and on an approximately linear line, in a position that gradually moves away from the line, depending on the water-rock interaction. While the cold-water sample plots on the meteoric line, $\delta^{18}O$ enrichment (positive shift) is observed for thermal waters. This situation is interpreted as the $\delta^{18}O$ change caused by water-rock interactions at long-term and high temperatures. Reservoir temperature, rock composition, and residence time affect the amount of oxygen exchange (Truesdell and Hulston, 1980).

The $\delta^{18}O$-Cl graph shows that there is a positive correlation between oxygen-18 and chloride (Figure 6). This shows us evaporative enrichment or the salinization of groundwater in the aquifer (reservoir) system by the effect of seawater. A slight $\delta^{18}O$ shift in the Bademli thermal spring water sample is interpreted as the result of processes of both evaporation and salinization. Because this spring occurs at the sea bottom near the coast. Therefore, the evaporation process is very common for the Bademli thermal spring.

4.3. Geothermometry applications

Chemical geothermometers are used to estimate the underground temperature of geothermal resources. These geothermometers give the final equilibrium temperature dependent on temperature (Nicholson, 1993). Of these geothermometers, numerical chemical ones were developed based on solubility and ion exchange. Fournier (1979) stated that thermal waters rise at a low speed towards the surface and change the direction of movement of some of them at shallow depths before reaching the surface or gaining horizontal flow, resulting in the thermal water losing its heat conductively and being cooled by the host rocks. Thermal waters can also cool down as a result of boiling or mixing cold groundwater due to sudden pressure changes at depths or when rising to the surface. The silica geothermometer is prepared based on the aquifer temperature affecting the chemical reaction or the cooling of the hot water as it rises. Therefore, silica geothermometry has been developed for various temperatures.

Solute geothermometry techniques were applied to thermal water samples in the study area (Table 4).

When some cation geothermometer results are discarded due to the seawater mixing process, it gives reservoir temperatures between 127 °C and 240 °C for the Bademli spring, and 130 °C and 246 °C for Hayıtlı region compared to the rest of the geothermometers (Table 4).

The Na-K-Mg triangle diagram is used to determine the origin of geothermal waters, to check whether they have reached equilibrium or not, and to select suitable geothermometers. With the Na-K-Mg geothermometer developed by Giggenbach (1988), both the reservoir

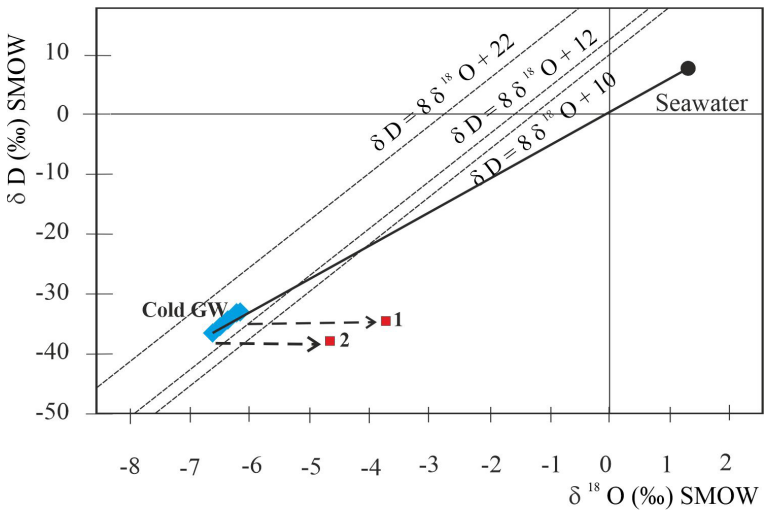

Figure 5. δ^2D-δ^{18}O diagram for study area (MMWL: Mediterranean meteoric water line (Yurtsever, 1986); LMWL: Local meteoric water line (Dilaver et al., 2018); GMWL: Global meteoric water line (Craig, 1961)).

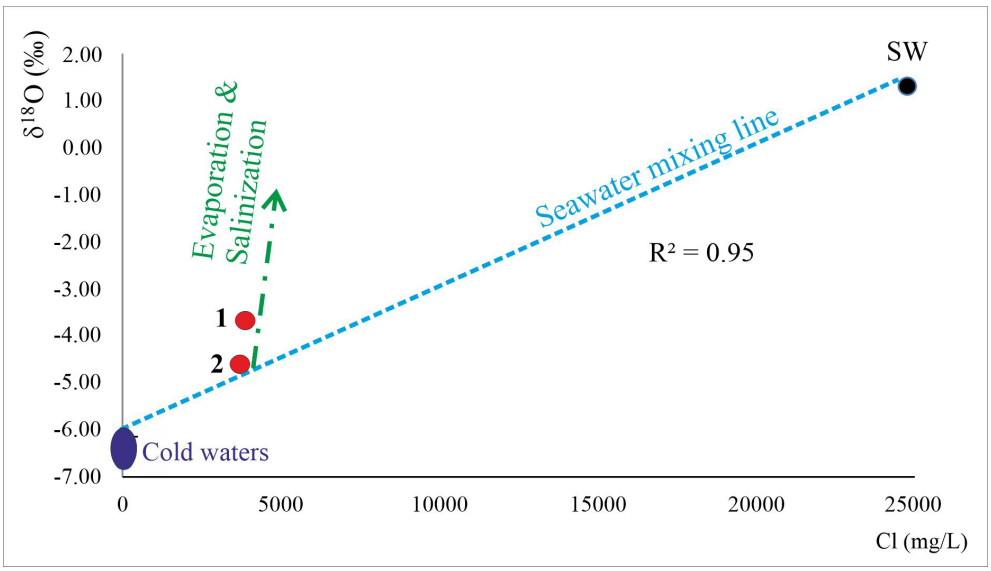

Figure 6. δ^{18}O-Cl diagram for the study area.

temperature of the geothermal water is determined and the accuracy of the cation geothermometer application is checked. Giggenbach's (1988) triangle diagram is a method used to distinguish between mature waters that have reached equilibrium with hydrothermal minerals and immature waters that are affected by mixing and/or rebalancing at low temperatures along circulation paths (Tarcan and Gemici, 2003). Cold-water samples fall into the immature field on this plot not attained mineral-rock equilibrium. Samples 1 and 2 plot as partially equilibrated waters but are also close to immature waters in Figure 7. It can be suggested that these water samples are also not a good representative of water-rock interactions in the reservoir. This can explain why some of the geothermometers give unreasonable geothermometry temperatures in Table 4. Most of the Na-K geothermometers give much higher than possible reservoir temperatures for the field. Because of the contribution of seawater and rapid water circulation in the system, the Na-K geothermometers may not reflect the reservoir temperatures. It can be said that these waters are not in full equilibrium with the reservoir rocks. In addition, most cation geothermometer results can only be considered tentative, due to the predominance of mixing thermal waters with seawater and/or cold groundwater.

Table 4. Results of chemical geothermometers (a-Fournier, 1977; b- Arnorsson, 1983; c- d Fournier & Truesdell, 1973; e- Fournier, 1979; f- Fournier & Potter, 1979; g- Tonani, 1980; h- Nieva & Nieva, 1987; i- Giggenbach, 1988; j-Giggenbach et at., 1983)

Sample Location	Bademli spring	Hayıtlı borehole
Discharge temperature (°C)	36.8	51
a- SiO_2 (Amorphous silica)	54	56
a- SiO_2 (a-cristobalite)	127	130
a- SiO_2 (b-cristobalite)	78	80
a- SiO_2 (Chalcedony)	156	158
a- SiO_2 (Quartz)	177	180
a- SiO_2 (Q-max. Steam loss)	166	168
b- SiO_2 (Chalcedony-conductive cooling)	150	153
b- SiO_2 (Quartz-steam loss)	144	147
b- SiO_2 (Quartz-steam loss)	151	154
b- SiO_2 (Quartz-steam loss)	172	174
b- SiO_2 (Quartz-steam loss)	165	167
b- SiO_2 (Chalcedony)	150	152
b- Na/K	178	182
b- Na/K	202	205
c- Na/K	164	169
d- Na/K	169	174
e- Na/K	202	206
b- Na/K	240	246
f- Na/K	221	225
g- Na/K	176	180
h- Na/K	190	193
i- Na/K	219	222
j- K/Mg	129	138

Reservoir temperatures calculated from silica and K-Mg geothermometers are more acceptable than other cation geothermometers. K-Mg geothermometry (Giggenbach et al., 1983) is useful in seawater mixing systems because Na and Ca are not equilibrated fast enough in the seawater mixing process (Henley et al, 1984). In this respect, the K-Mg geothermometer gave a more reliable reservoir temperature result since there is seawater contribution in BGA.

In the mineral-equilibrium method, the saturation of the minerals in the thermal water at certain temperature values is calculated separately. The saturation index lines corresponding to the temperature values marked on the diagram are interpreted. If a group of mineral lines crosses the equilibrium line (SI = 0) around a certain temperature value, the temperature value corresponding to the intersection of these lines gives the best aquifer temperature (Tarcan 2002) because the solubility equilibrium constants of minerals are closely related to temperature. Using the PHREEQC computer program, saturation indices (SI = log Q / K = log AP/Kt) at various temperatures (at 1 atm pressure condition) for each mineral were calculated separately. According to the temperature-mineral balance diagrams of the BGA thermal waters (Figure 8), the temperature values between 80–140 °C, where the curves intersect in the approximate equilibrium state, can be interpreted as the reservoir temperatures of the region.

Mixing models can be used to determine the reservoir temperature of a new geothermal field. Geothermal waters can mix with other waters as they rise to the surface. Assuming that the amount of silica is preserved as it was at the origin of the geothermal water, mixing ratios; maximum reservoir rock temperature can be explained by the change of enthalpy-silica (Fournier, 1977). The enthalpy-silica mixture model of the geothermal waters in the study area (Figure 9) suggests reservoir temperatures of approximately 240 °C for the Bademli spring and 208 °C for the Hayıtlı borehole, according to quartz geothermometry.

5. Conclusion and recommendation

BGA, which is a promising area in terms of thermal tourism and can be operated economically, has been evaluated in terms of hydrogeochemical and isotopic within the scope of this study. The reservoir rock of this geothermal area is the Lower-Middle Miocene-aged Dikili group volcanic rocks consisting of andesite, dacite, and basaltic andesite, which gained secondary permeability due to the tectonics. The N-S trending normal faults, which are important for BGA, and the strike-slip faults with oblique components, which cut these structures approximately perpendicularly, serve as the heat source of the system. Upper Miocene-Lower Pliocene aged sedimentary sequence represented by clayey limestone, limestone, cherty limestone, clay, marl, and siltstone with pyroclastic intercalations and chert level forms the cover rock of the system (Figure 10).

The thermal waters in BGA are of Na-Cl water type and their seawater contribution varies between 16%–18%. When the $\delta^{18}O$ and $\delta^{2}H$ values of the waters in the study area are examined, $\delta^{18}O$ enrichment can be seen, especially in the thermal waters. This is proof that the thermal system is a long-term and deep circulation system.

The outlet temperature of Bademli spring was 36.8 °C, and the wellhead temperature of the Hayıtlı borehole was 51 °C. According to the borehole information, the temperature measurement at the bottom of the well at a depth of 160 m rises up to 96 °C. According to various geothermometer calculations, reservoir temperatures vary between 80 and 240 °C. The Si-enthalpy graph may not

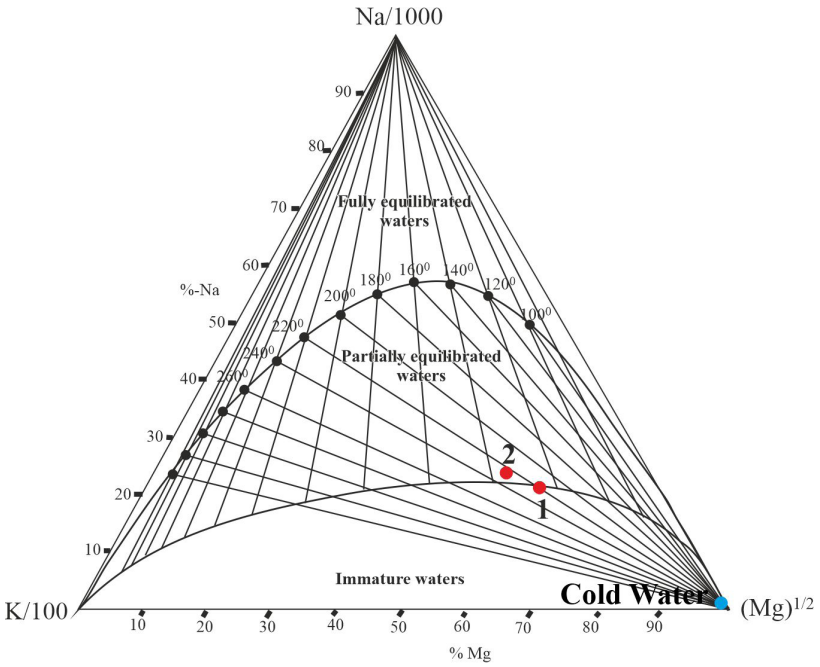

Figure 7. Distribution of the thermal waters from the BGA in a Na-K-Mg trilinear diagram.

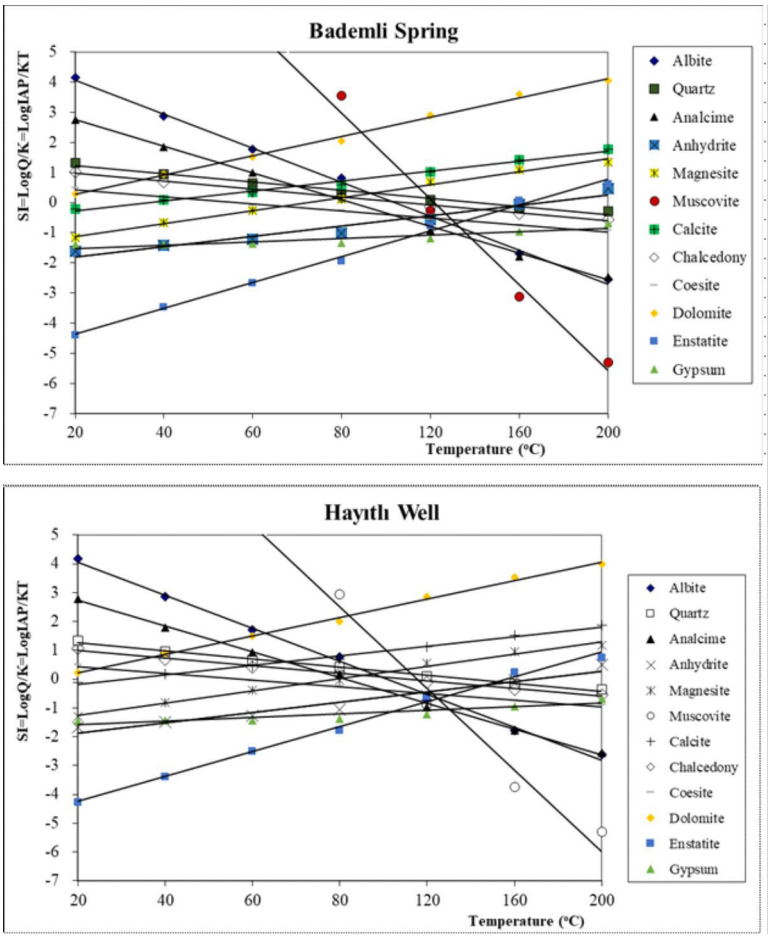

Figure 8. Mineral equilibrium diagrams for fluids.

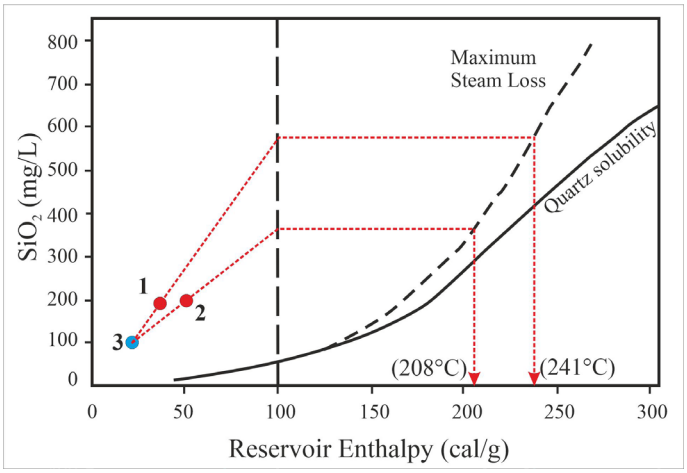

Figure 9. Reservoir enthalpy vs. SiO_2 diagrams based on quartz solubility for BGA.

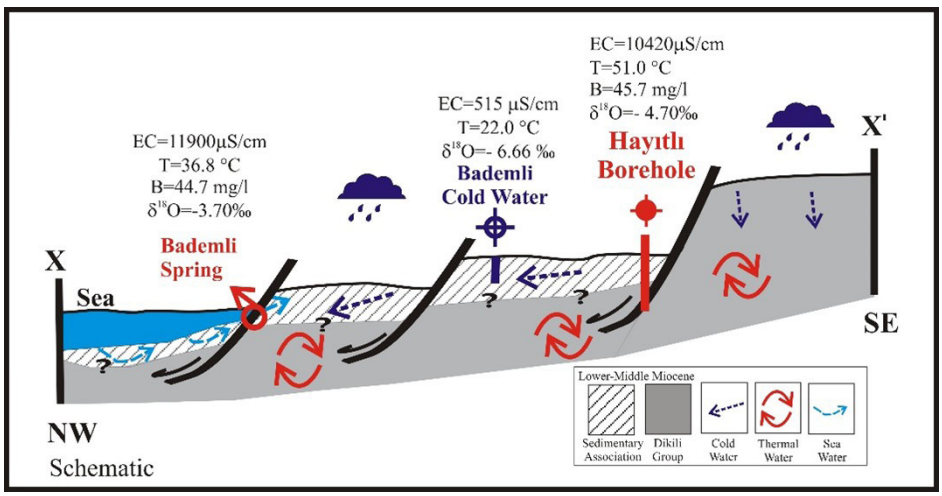

Figure 10. Hydrogeological conceptual model of BSA.

be accurate due to the seawater mixture. One of the most reliable geothermometers is K/Mg. Accordingly, Bademli spring gives a reservoir temperature of 129 °C and Hayıtlı borehole gives a reservoir temperature of 138 °C (Table 4).

Due to the high concentration of B, Fe, Mn, and Sb, the uncontrolled release of thermal water to the receiving medium can cause a major environmental problem.

Since this region is of great importance, especially in terms of thermal tourism, it is also important to determine new borehole areas. For BGA, it will be possible to get 96 °C high-temperature fluids with deep borehole wells to be made at the intersection points of N-S dip-slip faults and approximately E-W directional faults that cut these faults at an approximately right angle (Figure 10).

Acknowledgment

This project was funded as the project numbered 12.KB. FEN.089 of Dokuz Eylül University Scientific Research Projects (BAP). The authors thank Geological Engineers Pınar Akkoç Güneş, Umut Özdemir, Gülşah Bahçıvan Falay, and Doğu Şahan Vurkır for the support given during field studies.

References

Akar T, Gemici Ü, Somay-Altas M, Tarcan G (2021). Numerical modeling of fluid flow and heat transfer in kurşunlu geothermal field-kgf (Salihli, Manisa/Turkey). Turkish Journal of Earth Sciences. Volume 30, Issue SI-2: 1096 – 1111. https://doi.org/10.3906/yer-2106-12

Aksoy N (2014). Power generation from geothermal resources in Turkey. Renewable Energy, 68 (C): 595-601. https://doi.org/10.1016/j.renene.2014.02.049

Akyürek A, Soysal Y (1983). Biga yarımadası güneyinin (Savaştepe-Kırkağaç-Bergama-Ayvalık) temel jeoloji özellikleri. MTA Bulletin 95/96: 1–12 (in Turkish).

Alçiçek H, Bülbül A, Brogi A, Liotta D, Ruggieri G et al. (2018). Origin, evolution and geothermometry of the thermal waters in the Gölemezli Geothermal Field, Denizli Basin (SW Anatolia, Turkey). Journal of Volcanology and Geothermal Research 349: 1–30. https://doi.org/ j.jvolgeores.2017.07.021

APHA-AWWA-WPCF 3110 (1992). Standard methods for examination of water and wastewater, 18th eds. APHA-AWWAWPCF, Washington, DC.

Arnorsson S, Gunnlaugsson E, Svavarsson H (1983). The chemistry of geothermal waters in Iceland. III. Chemical geothermometry in geothermal investigations. Geochim.Cosmoschim. Acta 47: 567-577.

Ataberk E, Baykal F (2011). Utilization of natural and cultural resources of Dikili (Izmir) for tourism. Procedia Social and Behavioral Sciences 19: 173-180. https://doi.org/j.sbspro.2011.05.121

Baba A, Özgener L, Hepbasli A (2006). Environmental and exergetic aspects of geothermal energy. Energy Sources, Part A: Recovery, Utilization and Environmental Effects 28 (7): 597 –609. https://doi.org/10.1080/009083190928074

Balderer W, Synal HA (1996). Application of the chlorine-36 method for the characterization of the groundwater circulation in tectonically active areas: Examples from northwestern Anatolia/Turkey. Terra Nova 8 (4): 324 – 333.

Bardet, J (1914). Extraction du germanium des eaux de Vichy. Comptes rendus de l'Acade´mie des sciences 158: 1278–1280 (in French).

Bulut M, Filiz Ş (2005). Hydrogeological, hydrochemical and isotopic survey of the Bayındır geothermal area (İzmir, Western Anatolia, Turkey). Bulletin of the Mineral Research and Exploration 131 (131): 21-36. https://dergipark.org.tr/tr/pub/bulletinofmre/issue/3950/52391

Bülbül A, Özen T, Tarcan G (2011). Hydrogeochemical and hydrogeological investigations of thermal waters in the Alasehir-Kavaklidere area (Manisa-Turkey). African Journal of Biotechnology 10 (75): 17223–17240. https://doi.org/10.5897/AJB11.3050

Calmbach L (1997). AquaChem Computer Code-Version 3.7.42. Waterloo Hydrogeologic, Waterloo, ON.

Çetin G, Özkaraca O, Keçebaş A (2021). Artificial neural network-based optimization of geothermal power plants. Thermodynamic Analysis and Optimization of Geothermal Power Plants pp: 263-278. https://doi.org/10.1016/B978-0-12-821037-6.00008-1

Craig H (1961). Isotopic variations in meteoric waters. Science 133:1702– 3

Demirel F (1993). Bademli-Dikili bölgesinin hidrojeolojisi. Dokuz Eylül Üniversitesi Jeoloji Mühendisliği Bitirme Tezi (Unpublished) (in Turkish).

Dilaver AT, Aydın B, Özyurt NN, Bayarı CS (2018). Türkiye Yağışlarının İzotop İçerikleri (2012-2016), DSİ-TAKK ve MGM-AD, Ankara, 44 s DMİ, 2016. Elazığ Bölge Müdürlüğü İstasyon Raporu, Devlet Meteoroloji Genel Müd., Ankara (in Turkish).

Dobrzynski D, Boguszewska-Czubara A, Sugimori K (2018). Hydrogeochemical and biomedical insights into germanium potential of curative waters: a case study of health resorts in the Sudetes Mountains (Poland). Environ Geochem Health 40: 1355–1375. https://doi.org/10.1007/s10653-017-0061-0

Eşder T, Şimşek Ş (1977). The relationship between the temperature-gradient distribution and geological structure in the Izmir-Seferihisar Geothermal Area, Turkey. In: Proc. of the Symp. on the Geothermal Energy, Ankara, pp. 93-114.

Filiz Ş (1982). Ege Bölgesindeki Önemli Jeotermal alanların ^{18}O, ^{2}H, ^{3}H, ^{13}C izotoplarıyla incelenmesi (in Turkish). Assoc.Prof. Thesis. E.U.Y.B.F., İzmir.

Filiz S, Tarcan G (1990). Gülbahçe Körfezi güneyindeki jeotermal alanın hidrojeolojik, hidrojeokimyasal ve izotopsal incelenmesi, Turkish Association of Petroleum Geologist Bulletin 2 (1): 69–52 (in Turkish).

Filiz Ş, Tarcan G (1997). High boron content in the aquifer system of the Gediz Basin (on the Aegean region of Turkey). IESCA-1995 Proceedings, 2: pp 681–692.

Filiz Ş, Tarcan G, Gemici Ü (1998). Dikili–Bergama (İzmir) Jeotermal Alanları'nın Hidrojeolojik İncelenmesi, Türkiye Madencilik Kongresi, 2-6/Kasım/1998, MTA- Ankara, Bildiri Metinleri Kitabı (2000), pp: 487-508 (in Turkish).

Fournier RO (1977). A review of chemical and isotopic geothermometers for geothermal systems. Proceedings of the Symp. on Geothermal Energy. Cento Scienti¢c Programme, Ankara, pp. 133-143.

Fournier RO (1979). A revised equation for the Na-K geothermometer. Geotherm. Res. Counc. Trans. 3: 221-224.

Fournier RO, Truesdell AH (1973). An empirical Na-K-Ca geothermometer for natural waters. Geochimica et Cosmochimica Acta 37: 1255-1275.

Fournier RO, Potter RW (1979). Magnesium correction to the Na-K-Ca chemical geothermometer. Geochimica et Cosmochimica Acta 43: 1543-1550.

Gemici Ü, Filiz Ş (2001). Hydrochemistry of the Çeşme geothermal area, Turkey. Journal of Volcanology and Geothermal Research 110: 171-188. https://doi.org/10.1016/S0377-0273(01)00202-5

Gemici Ü, Tarcan G (2002). Distribution of boron in thermal waters of western Anatolia, Turkey and examples on their environmental impacts. Environmental Geology 43: 87–98. https://doi.org/10.1007/s00254-002-0608-x

Gemici Ü, Tarcan G, Çolak M, Helvacı C (2004). Hydrogeochemical and hydrogeological investigations of thermal waters in the Emet area (Kütahya, Turkey). Applied Geochemistry 19 (1): 105–117. https://doi.org/10.1016/S0883-2927(03)00112-4

Gönenç T, Pamukçu O, Pamukcu C, Deliormanlı AH (2012). The investigation of hot spots in western Anatolia by geophysical and mining approaches. Energy Sources, Part A: Recovery, Utilization and Environmental Effects 34 (9): 775–792. https://doi.org/10.1080/15567031003627914

Giggenbach WF (1988). Geothermal solute equilibria. Derivation of Na-K-Mg-Ca geoindicators. Geochimica et Cosmochimica Acta 52: 2749-2765.

Giggenbach WF (1991). Chemical techniques in geothermal explanations. In: D'Amore F (coordinator) Application of geochemistry in geothermal reservoir development. UNITAR/ UNDP Publications, Rome, pp 119–142.

Giggenbach WF, Gon¢antini R, Jangi BL, Truesdell AH (1983). Isotopic and chemical composition of Parbati Valley geothermal discharges, NW Himalaya, India. Geothermics 5: 51-62.

Güleç N (1988). The distribution of helium-3 in western Turkey. Bulletin of the Mineral Research and Exploration (MTA Dergisi) 108: 35–42.

Henley RW, Truesdell AH, Barton PB, Whitney JA (1984). Fluid-Mineral Equilibria in Hydrothermal Systems. Reviews in Economic Geology, vol. 1.

IAH (International Association of Hydrogeologists) (1979). Map of mineral and thermal water of Europe. Scale 1:500,000. International Association of Hydrogeologists, United Kingdom.

İZKA (İzmir Kalkınma Ajansı) (2022). İzmir İlindeki Jeotermal Kaynakların Potansiyeli, Kullanım Alanları, Ekonomik ve Çevresel Etkilerinin Belirlenmesi Araştırması, İzmir Kalkınma Ajansı (in Turkish).

Karacık Z, Yılmaz Y, Pearce JA (2007). The Dikili-Çandarlı volcanics, western Turkey: magmatic interactions as recorded by petrographic and geochemical features. Turkish Journal of Earth Sciences 16: 493–522.

Karamanderesi İH (1997). Geology and hydrothermal alteration processes of the Salavatlı-Aydın geothermal field. PhD thesis, Dokuz Eylul University, İzmir, Turkey (Unpublished).

Koga A (1967). Germanium, molybdenum, copper and zinc in New Zealand thermal waters. New Zealand Journal of Science 10: 428–446.

Kuroda K (1939). The occurrence of germanium in the hot springs of Senami. Bulletin of the Chemical Society of Japan 14 (7): 303–304.

MAPEG (2022). Türkiye Jeotermal Kaynaklar Strateji Raporu. Maden ve Petrol İşleri Genel Müdürlüğü (in Turkish).

Mutlu H, Güleç N, Hilton DR (2008). Helium-carbon relationships in geothermal fluids of western Anatolia, Turkey. Chemical Geology 247 (1-2): 305–321. https://doi.org/10.1016/j.chemgeo.2007.10.021

Magri F, Akar T, Gemici Ü, Pekdeğer A (2011). Numerical investigations of fault-induced seawater circulation in the Seferihisar-Balçova geothermal system, western Turkey. Hydrogeology Journal 20: 103-118. https://doi.org/10.1007/s10040-011-0797-z

Nicholson K (1993). Geothermal Fluids; Chemistry and Exploration Techniques. Springer, Berlin.

Nieva D, Nieva R (1987). Developments in Geothermal Energy in Mexico Part 12. A Cationic Composition Geothermometer for Prospecting of Geothermal Resources. Heat Recovery Systems and CHP 7: 243-258.

Özen T, Tarcan G (2005). Dikili-Kaynarca (İzmir) Jeotermal Sistemlerinin Hidrojeolojik ve Jeokimyasal Değerlendirilmesi. Dokuz Eylül Üniversitesi Mühendislik Fakültesi Fen ve Mühendislik Dergisi 7 (2): 87-100. (in Turkish) https://dergipark.org.tr/tr/pub/deumffmd/issue/40872/493473

Özen T, Bülbül A, Tarcan G (2012). Reservoir and hydrogeochemical characterizations of geothermal fields in Salihli, Turkey. Journal of Asian Earth Sciences 60: 1-17. https://doi.org/10.1016/j.jseaes.2012.07.016

Özgür N (2002). Geochemical signature of the kizildere geothermal field, Western Anatolia, Turkey. International Geology Review 44 (2): 153–163. https://doi.org/10.2747/0020-6814.44.2.153

Pasvanoğlu S (2020). Geochemistry and conceptual model of thermal waters from Erciş - Zilan Valley, Eastern Turkey. Geothermics 86: Article 101803. https://doi.org/10.1016/j.geothermics.2020.101803

Özkan R, Şener M, Helvacı C (2011). Aliağa (İzmir) jeotermal alanındaki hidrotermal alterasyonlar ve termal sularla ilişkisi. Yerbilimleri/ Earth Sciences. 32 (1): 1–20 (in Turkish).

Parkhurst DL, Appelo CAJ (1999). User's Guide to PHREEQC (Version 2) - A Computer Program for Speciation, Batch-Reaction, One-Dimensional Transport, and Inverse Geochemical Calculations.

Richards LA (1954). Diagnosis and Improvement of Saline Alkali Soils, Agriculture, 160, Handbook 60. US Department of Agriculture, Washington DC.

Somay M, Gemici Ü, Filiz S (2008). Hydrogeochemical investigation of Kucuk Menderes River coastal wetland, Selcuk–Izmir, Turkey. Environmental Geology 55: 149-164. https://doi.org/10.1007/s00254-007-0972-7

Şimşek Ş (1985). Geothermal model of Denizli, Sarayköy-Buldan area. Geothermics 14: (2-3): 393 – 417.

Tarcan G, Gemici Ü (2003). Water geochemistry of the Seferihisar geothermal area, İzmir, Turkey. Journal of Volcanology and Geothermal Research 126: 225-242. https://doi.org/10.1016/S0377-0273(03)00149-5

Tarcan G, Gemici Ü, Aksoy N (2005). Hydrogeological and geochemical assessments of the Gediz Graben geothermal areas, western Anatolia, Turkey. Environmental Geology 47 (4): 523–534. https://doi.org/10.1007/s00254-004-1174-1

Tarcan G, Gemici Ü, Aksoy N (2009). Hydrogeochemical factors effecting the scaling problem in Balçova geothermal field, İzmir, Turkey. Environmental Geology 58 (7): 1375 – 1386. https://doi.org/10.1007/s00254-008-1640-2

Truesdell AH, Hulston JR (1980). Isotopic evidence on the environments of geothermal systems. In: Fritz P, Fontes, JC (Eds.), Handbook of Environmental Isotope Geochemistry. Elsevier, New York, pp. 179-226.

Tonani F (1980). Some Remarks on the Application of Geochemical Techniques in Geothermal Exploration. Proceedings of the 2nd International Seminar on the Results of EC Geothermal Energy Research, Strasbourg, 4-6 March 1980, pp. 428-443. https://doi.org/10.1007/978-94-009-9059-3_38

Tut-Haklıdır FS, Özen-Balaban T (2019). A review of mineral precipitation and effective scale inhibition methods at geothermal power plants in West Anatolia (Turkey). Geothermics 80: 103–118. https://doi.org/10.1016/j.geothermics.2019.02.013

Wood SA, Samson IM (2006). The aqueous geochemistry of gallium, germanium, indium and scandium. Ore Geology Reviews. 28: 57–102. https://doi.org/10.1016/j.oregeorev.2003.06.002

Vengosh A, Helvacı C, Karamanderesi İH (2002). Geochemical constraints for the origin of thermal waters from western Turkey. Applied Geochemistry 17: 163-183. https://doi.org/10.1016/S0883-2927(01)00062-2

Yang Yi, Huo Yaowu, Xia Wenkai, Wang Xurong et al (2017). Construction and preliminary test of a geothermal ORC system using geothermal resource from abandoned oil wells in the Huabei oilfield of China. Energy 140: 633-645. https://doi.org/10.1016/j.energy.2017.09.013

Yılmazer S (1984). Ege Bolgesi'ndeki bazı sıcak su kaynaklarının hidrojeoloji ve jeokimyasal incelemeleri. D.E.U. Fen Bilimleri Enstitusu, MSc. Thesis, İzmir. (in Turkish)

Yurtsever Y (1983). Models for tracer data analysis. In: Guidebook on nuclear techniques in hydrology. Technical Report. Series no. 91, IAEA, Vienna.